Journal of Mines, Metals and Fuels, *73(3): 815-827; 2025. DOI: 10.18311/jmmf/2025/47519*

Print ISSN : 0022-2755

Journal of Mines, Metals and Fuels

**Contents available at:** *www.informaticsjournals.co.in/index.php/jmmf*

# A Study Employing the Taguchi Approach, Regression Analysis, and Artificial Neural Network to Analyze the Performance of a Single-Cylinder Piston-Type Compressed Air Engine

**Lalit S. Patel[1,5]*, Viral P. Parekh[2,5], Balvant C. Patel[3,5], Hardik H. Makwana[4,5] and Ratnesh K. Shukla[1,5]**

*[1]Mechanical Engineering Department, Dr. S and S. S. Ghandhy Government Engineering College, Surat - 395001, Gujarat, India; lspatel82rp@gmail.com*

*[2]Mechanical Engineering Department, Sardar Vallabhbhai Patel Institute of Technology, Vasad - 388306, Gujarat, India*

*[3]Mechanical Engineering Department, Government Engineering College, Valsad - 396001, Gujarat, India*

*[4]EC Engineering Department, Dr. S and S. S. Ghandhy Government Engineering College, Surat - 395001, Gujarat, India*

*[5]Gujarat Technological University, Ahmedabad - 382424, Gujarat, India*

## Abstract

*Researchers are looking for new energy sources or ways to optimize energy use because of the overuse of fossil fuels. In order to lessen the amount of carbon footprint in the atmosphere, a lot of research is being done on creating more environmentally friendly and efficient methods of producing the energy needed for propulsion. In order to create a cleaner, more sustainable, and emission-free future, this work presents a physical model of a Compressed Air Engine (CAE), which is established from an existing 4-stroke, 100-CC petrol engine. To achieve performance on CAE, a traditional four-stroke internal combustion engine that had been scrapped was converted to a two-stroke compressed air engine. Through experimental research, the output torque and brake power are determined. Through the use of experiment design, on a test bench of the piston type compressed air engine, the brake power has been examined under various loading scenarios. The L9 Taguchi method is utilized for parametric analysis and experimentation in experiment design. Regression analysis was used in the development of the mathematical model. Confirmation runs show that the results derived from Artificial Neural Networks (ANNs) and regression analysis match with the optimized values. The findings demonstrate that CAE operates economically at 5 kg/cm$^2$ of pressure and can produce up to 0.93 kW of power at varying loads of 1.5 kg to 2.5 kg.*

***Major Findings:*** *The findings demonstrate that the compressed air engine which was a 4-stroke single-cylinder internal combustion engine was converted into a 2-stroke air engine by modifying the cam operates economically at 5 kg/cm$^2$ of pressure and can produce up to 0.93 kW of power at varying loads of 1.5 kg to 2.5 kg.*

**Keywords:** *Brake Power, Cam Design of Experiment, Internal Combustion Engine, Piston Type*

**Author for correspondence*

## 1.0 Introduction

Realizing the effects of unconditioned pollution, fog, acid rain, greenhouse effect, ozone layer depletion, and other environmental threats on human health, believers of eco-friendly development have been pushing the idea of sustainable development over the past ten years. Therefore, engineers everywhere are focusing on the creation and application of using renewable energy instead of fossil fuels[1]. Individuals search for alternate energy sources due to environmental damage and the consumption of fossil fuels[2,3]. Ideal solutions are found in the use of renewable fuels like compressed air, solar power, and wind[4]. To adequately address the challenges of sustainable energy development, a broad spectrum of renewable energy technologies must be available[5]. The advantages of compressed-air vehicles include their low cost and zero pollution[6]. Energy storage equipment is crucial for the growth of distributed power, intelligent grids, and the energy-efficient Internet[7,8]. Air pollution has become a serious issue endangering human progress and survival[9]. Shafi and Topale predict that by 2042, the quantity of oil and gas reserves will be reduced in order to conserve the environment. This renewable energy will boost competition in the automotive industry[10]. Given that a large portion of the world's primary energy demand is accounted for by transportation as well as that internal combustion engine exhaust contributes substantially to carbon emissions[11,12]. To offer an example, a 2009 UCS research in the United States projected that a national renewable energy consumption target of 25 percent by 2025 would reduce carbon dioxide emissions from power stations by 277 million metric tons yearly by that time. That amount is equivalent to the annual production from 70 standard (600 MW) freshly constructed coal plants[13]. From 0.6 and 2 pounds of carbon dioxide equivalent per kilowatt-hour ($CO_2E$/kWh) are released when burning natural gas for electricity, whereas between 1.4 and 3.6 pounds are published when burning coal. In comparison, wind results only 0.02 to 0.04 pounds of $CO_2E$/kWh over its life cycle; solar results 0.07 to 0.2; geothermal results 0.1 to 0.2; and hydroelectric results between 0.1 and 0.5[14]. Identifying sources of clean and ecologically sound energy alternatives is essential. Several types of zero-emission cars have been well studied. High energy efficiency, power system compensation, energy divergence, and flawless operation are provided by battery electric vehicles[15]. However, a number of the challenges that occur are limited life span development and application, heavy metal pollution, and high initial costs[16]. Despite the substantial energy content of hydrogen, problems with protection, storing, and energy efficiency are currently obstructing the development of fuel-cell automobiles made from hydrogen[17]. One potentially clean and eco-friendly energy source is compressed air. The energy density of compressed air is comparable to that of a lithium battery when the temperature and pressure are 300K and 30MPa, respectively[18]. Furthermore, the Compressed Air Engine (CAE) is reasonably less expensive and it takes less time to fully recharge the air tank[19,20].

In years to come, compressed air energy storage is expected to grow into an innovative and quickly transforming field because of its broadened lifespan, substantial energy storage density, affordable price, safe storage, ease of use, and reusability. Compressed air engines serving as the primary provider of power has been the subject of very few research studies and industrial projects[21]. *Liu* and *X Yu* used thermodynamic analysis and experimental data to examine the viability and future prospects of compressed air vehicles. The field of application and various energy storage techniques are introduced by H Ibrahim *et al*[22,23]. Transmission energy and relaxation energy are two categories into which the compressed air's energy can be separated. According to reference, the expansion energy ratio increases with air pressure[24]. India is among the developing nations with the fastest rates of economic growth, and as a result, there is frequently a greater need for transportation. The amount of fuel used is roughly in line with this demand. India's economy is greatly impacted by its heavy reliance on imported fuel due to a scarcity of fossil fuel reserves. India needs to find additional methods to keep up its growth rate. In India, around 53% of rural households and 93% of urban households have access to electricity. Thirty-five percent of Indians live without access to electricity[25]. A compressed air engine is a more reliable choice for generating electricity for devices like generators and cars. It doesn't require any known fossil fuels, including hydrogen, LPG, CNG, gasoline, or diesel[26]. It's crucial to keep in mind that, despite their seeming impossibility, vehicles powered solely by compressed air still pique the interest of the general public due to their environmentally

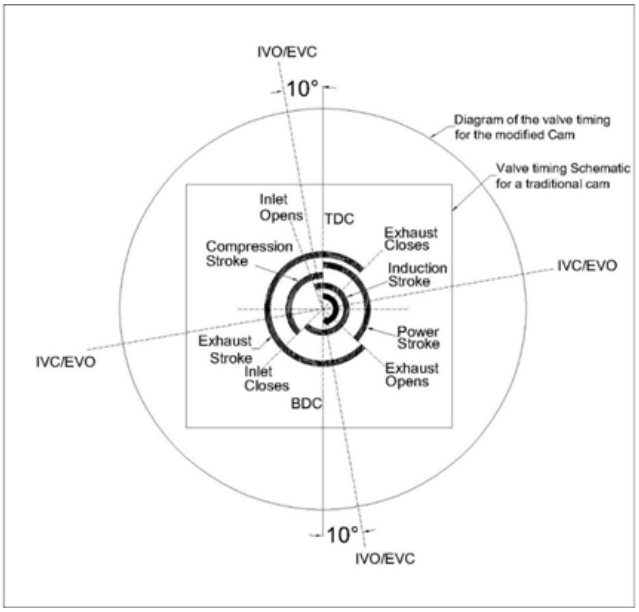



**Figure 1.** Diagram of the valve timing for the modified cam.

beneficial qualities. It should be a goal to make them lightweight, secure, affordable, and efficient. More care must be taken to ensure that compressed air is stored both initially and during the journey, with all of its advantages-such as no heating, high energy density, and the ability to utilize cooling created by adiabatic expansion during energy release. Already-available electric vehicles and bicycles pose a serious threat to compressed air vehicles, both in terms of price and environmental impact. Even though the technology seems a long way off, researchers are still working on it[27].

## 2.0 Experimental Methods

Compressed air vehicles terminate their cycle in a 2-stroke manner, which makes 4-stroke internal combustion engines unsuitable for them. Therefore, a change from 4-stroke to 2-stroke engines is required. Current research concentrates on influencing the valve timing mechanism. Cam profiling is a fundamental concept in the conversion of four-stroke engines to two-stroke engines. The valve timing diagrams for the modified and conventional cams are shown in Figure 1, and the dimensions and isometric view of the cam is labeled in Figure 2a and 2b. Before the testing, the abandoned 100 CC internal combustion engine, with a maximum power of 7.0 ps at 8000 rpm

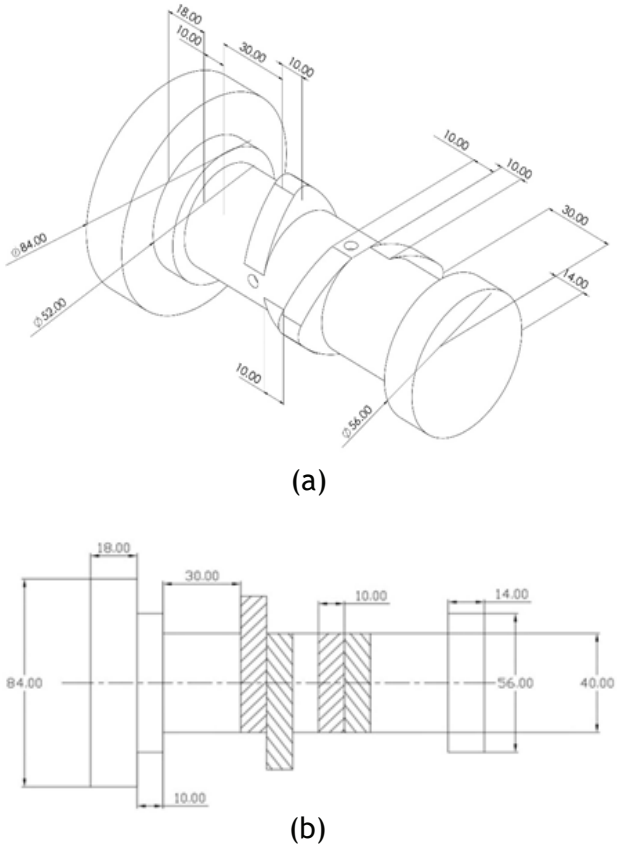



**Figure 2.** Detailed dimensions of modified cam with **(a)** Isometric view **(b)** Sectional view.

and a maximum torque of 7.5 nm, was modified and connected to a compressed air reservoir. The cam profile was conjugated to change the engine's functioning from four to two strokes. Following engine installation, the intake and exhaust valves were tested for any leaks during high air pressure operation.

Due to the intake valve's seepage being so close to the experiments flow rate, the compressed air engine's performance was negatively impacted. When there was an engine lockup while the intake process, the exhaust valve leakage was checked, and no leak was found. Figure 3 illustrates the experimental configuration for a single-cylinder air engine and Figure 4 shows the methodology of the whole research work.

## 3.0 Experimental Design

Establishing the parameters that are crucial and their target values is the aim of the experiments formation[28]. It

**Table 1.** Process parameter level

| Factor | Symbol | Unit | -1 | 0 | 1 |
|---|---|---|---|---|---|
| Air Pressure | p | $kg/cm^2$ | 4 | 5 | 6 |
| Load | L | kg | 1.5 | 2 | 2.5 |

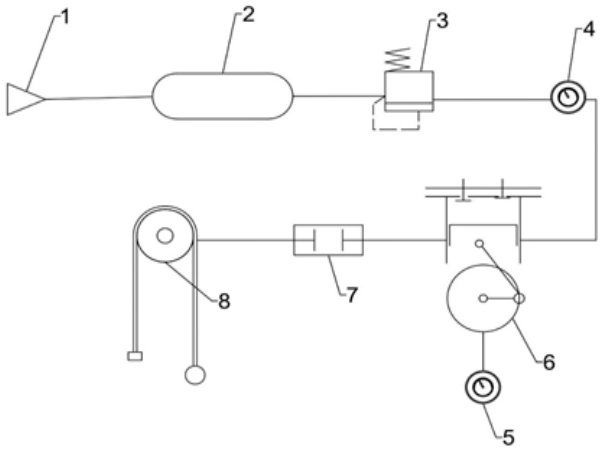



**Figure 3.** Configuration of experimental set up: **(1)** Compressor **(2)** Compressed air tank **(3)** Pressure regulator **(4)** Intake pressure gauge **(5)** CAE pressure gauge **(6)** Compressed air engine **(7)** Coupling **(8)** Rope brake dynamometer.

involves creating an experimental design based on chosen parameters. Among the most essential components of any experimental endeavor is the process parameters. For L9 OA, the Taguchi experimental design has been finalized for two variables: Different load cases, air pressure and brake power is the primary parameter used as a response in the present investigation. The process parameters in this instance are chosen after a review of numerous fragments of works. For air pressure and load operating on the compressed air engine, different levels of process parameters are shown in Table 1.

## 4.0 Results and Discussion

The rope brake dynamometer, made up of a brake drum, spring balance, belt, and holding frame, is connected to the air engine for load testing. Brake power was measured during testing using the Taguchi design of experiments L9 to ascertain the air pressure's effective parameters when loading is present.

### 4.1 Taguchi Analysis of an Air Engine's Braking Power in Relation to Pressure and Load

The selected characteristics average for each factor level is displayed in response Table 2 and Table 3. The response tables compare the relative magnitude of effects

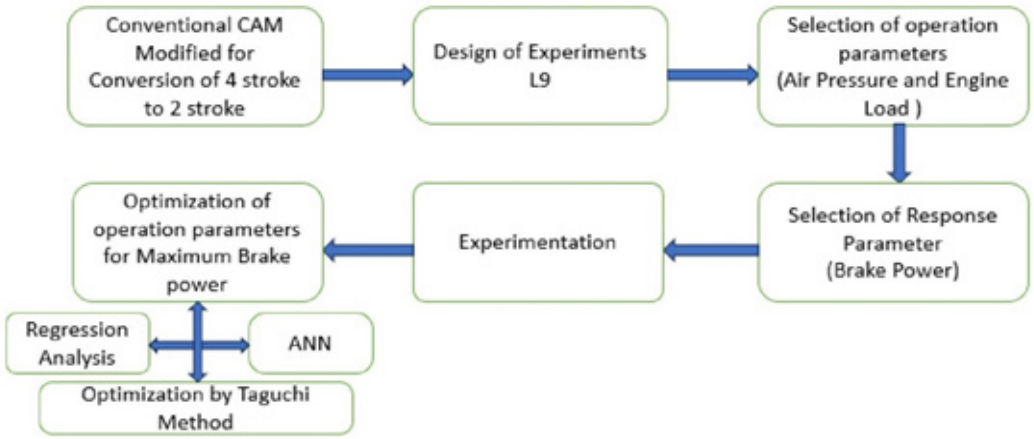



**Figure 4.** Methodology of the present research work.

and include ranks based on Delta statistics. The greatest average for every factor less the lowest average for each factor is the delta statistic. According to the analysis, load (delta = 3.6067, Rank = 1) has the largest impact on the S/N ratio; hence, load is given a greater weight than air pressure when it comes to brake power (Tables 2 and 3). Delta values are used to assign ranks; the highest Delta value is assigned to rank 1, the second highest to rank 2, and so forth. In the main effects plot, the mean of the response table charts is displayed. Figure 5 demonstrates that a rise in pressurized air pressure would end up resulting in more braking power, and inversely. The graph also demonstrates how braking power drops and rises inversely at decreasing load amounts. It is apparent from this that lowering the air under compression pressures during the intake process and reducing the load placed on the compressed air engine would result to a drop in braking power.

Figure 6 illustrates the interplay between brake power and load. It is dependent upon the pressure's value. Here, the combination is linked to a higher brake power, according to the plot at 2.5 kg load and 5 bar pressure. The brake power response diagram is displayed in Figure 7. It is obvious that increasing the load placed on an air-compressed engine and the compressed air pressure input parameters will increase brake power. This indicates that when engine load is increased, brake power increases significantly. Figure 8 shows the plot of the SN ratio for the influence of compressed air pressure on brake power compared to the load on the air engine. The results from the interaction plot for means show that higher brake power is achieved with compressed air pressure at 5 bar, matching the optimal condition of 2.5 kg load.

**Table 2.** Signal to noise ratio response table

| Level | Pressure (bar) | Load (kg) |
|---|---|---|
| 1 | -2.8946 | -4.5359 |
| 2 | -2.5634 | -2.3877 |
| 3 | -2.3953 | -0.9292 |
| Delta | 0.4994 | 3.6068 |
| Rank | 2 | 1 |

**Table 3.** Table of responses for means

| Level | Pressure (bar) | Load (kg) |
|---|---|---|
| 1 | 0.7288 | 0.5939 |
| 2 | 0.7575 | 0.7602 |
| 3 | 0.7664 | 0.8989 |
| Delta | 0.0375 | 0.3048 |
| Rank | 2 | 1 |

## 4.2 Analysis of Contour Plot

A contour plot is a type of graph used to investigate possible correlations between three different variables. With the response values represented by contours and the x- and y-factors (predictors) plotted on the x- and y-scales, contour plots show the three-dimensional relationship in two dimensions. A contour plot shows values for x, y, and z instead of longitude, latitude, and elevation, much like a topographical map does. The contours of a brake power are changed by pressure (y) and load (x), as demonstrated in Figure 9. Greater braking power is shown by the darker green spots. It is obvious from Figure 9 that the highest braking power, or darker green region in a convex form, is produced when 5 bar pressure and 2.5 kg weight are coupled. Given that this graph depicts the average braking power range, it will be relatively straight forward to anticipate the compressed air pressure under different loading situations for an air engine.

## 4.3 Verification of Findings

The experiment validation is the final step in establishing the results gained from Taguchi's parameter design technique. Designing parameters, the validation test is crucial, especially when conducting screenings or using small fractional factorial designs[28]. This research employed the braking power level of parameters to verify the experiment for the 4-stroke air compression test rig. Minitab 16 static program is used to do regression analysis and build regression equations for different factors. One way for studying the many sorts of connections among variables that are both independent and dependent is the method of regression analysis. Under some conditions,

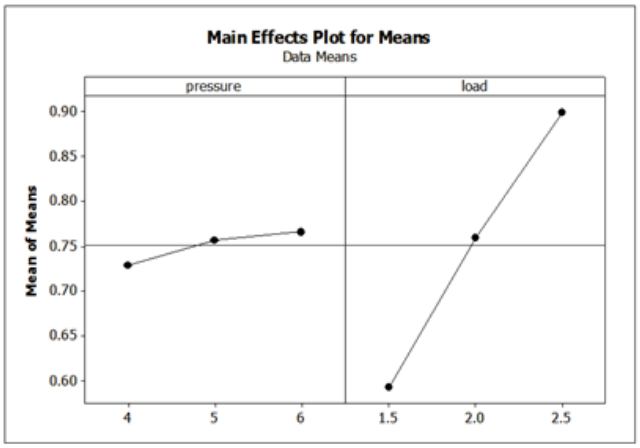



**Figure 5.** Main effect diagram for brake power means.

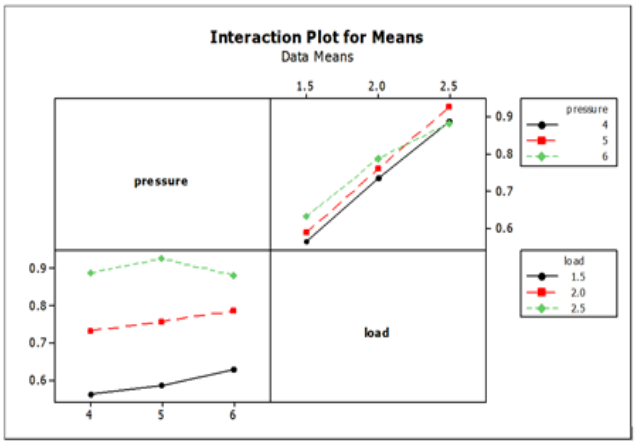



**Figure 7.** Main effect plot for SN ratio.

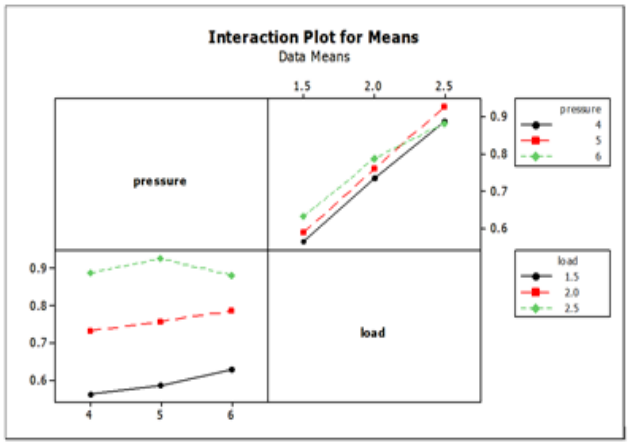



**Figure 6.** Main effect diagram for brake power means.

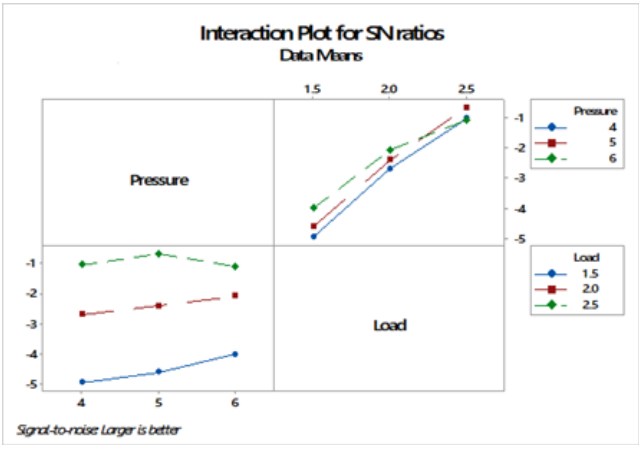



**Figure 8.** Brake power interaction plot of the SN ratio

regression analysis may assist find causal links among variables that are both independent and dependent. To assess the connections amongst parameters in mathematical predictive analysis is a set of statistical processes. Regression analysis is a valuable technique for prediction and data analysis.

## 4.4 The Linear Regression Approach

Linear regression is a well-known modeling approach that many folks start with when diving into predictive modeling. It works with a continuously dependent variable along with one or more discrete or continuous independent variables, generating a linear regression line[29,30]. By using a best-fit straight line, which is known as the regression line, a model based on linear regression discovers the link among the variable that is dependent (Y) and a set of independent variables (X).

## 4.5 regression analysis.

In this study, linear regression has been conducted using Minitab 16 statistical software. The connection between the input parameters, such as load and air pressure, and brake power had been determined.

Mean BP = 0.0474 + 0.0188 pressure + 0.306 load

Table 4 provides the results of braking power for experiments and regression equation for different loading circumstances as well as pressure ranges between 4 and 6 kg/cm$^2$. The interaction between brake power and compressed air pressure for a 1.5 kg load can be seen in Figure 10, using an equation for four-stroke air

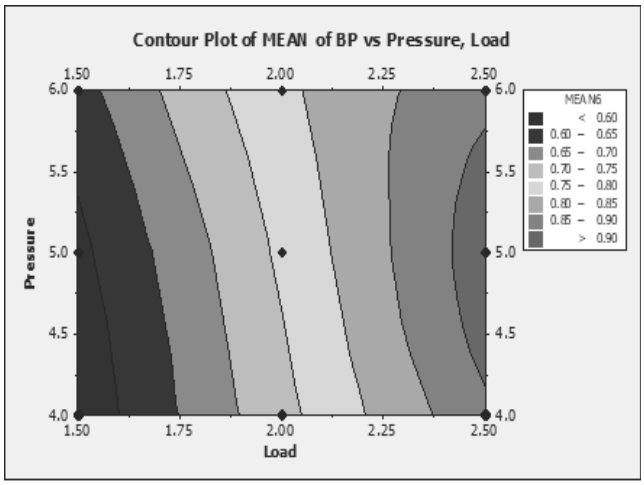



**Figure 9.** Contour plot for brake power mean vs pressure and load.

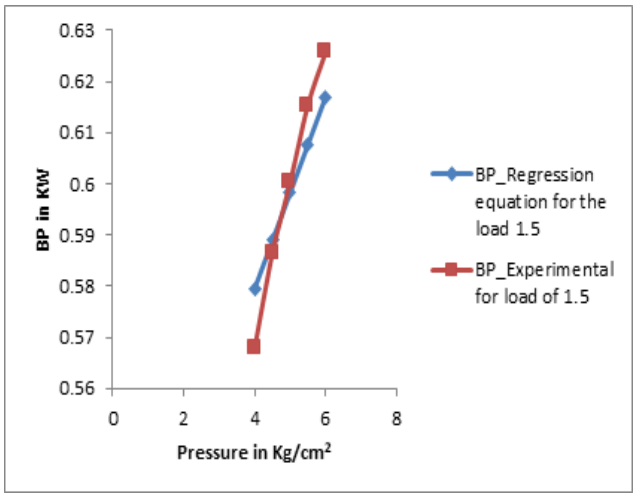



**Figure 10.** Brake power comparison plot at 1.5 kg load.

engines and experimental data. This figure shows that the equation and experimented brake power values for a 1.5 kg load are well matched. Additionally, it is evident that the maximum error between the equation and the experiments is approximately 2 percent for air pressures of 4 kg/cm$^2$. Brake power, calculated from equation and measured experimentally, can be seen in Figure 11. This figure indicates a close relationship between the measured and predicted brake power. For example, the maximum error between the equation and experiment is found to be approximately 1.96% at a pressure of 6 kg/cm$^2$.

Figure 12 demonstrates a comparison between experimental and equation-derived Brake power under

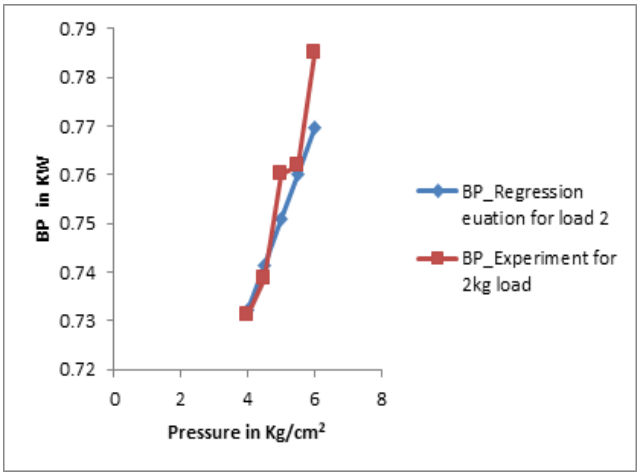



**Figure 11.** Brake power comparison plot at 2 kg load.

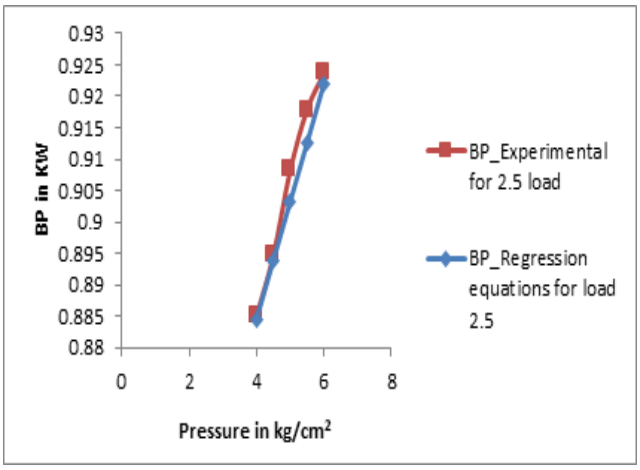



**Figure 12.** Brake power comparison plot at 2.5 kg of load.

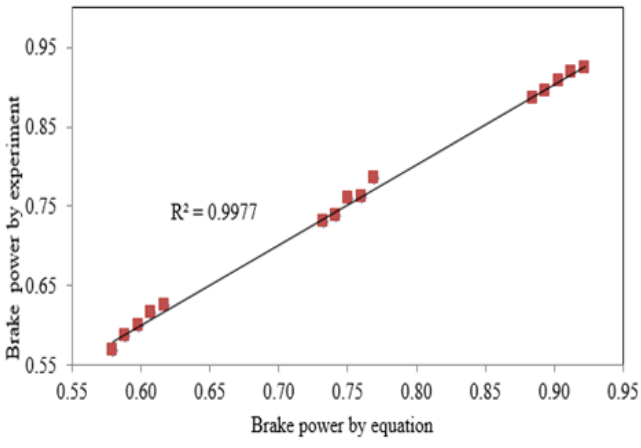



**Figure 13.** Brake power comparison plot between measured and predicted values.

varying pressure and a constant load of 2.5 kg. It is obvious from the graph that there is a solid correlation between the Brake power levels produced from both approaches.

Figure 13 compares the predicted and measured values of compressed air pressure (4 kg/cm$^2$ to 6 kg/cm$^2$) and brake power (1.5 kg to 2.5 kg) for the respective load ranges. Given that the R2 values on this graph are approximately close to one, it is evident that the brake power numbers given by the equation and the tests are compatible with one another.

## 4.6 Artificial Neural Networks (ANN)

ANNs, or artificial neural networks, are an effective substitute for measuring the air engines performance and B.P[31,32]. The model's nodes take in inputs like load and air pressure, process them, and determine the activation value or outputs in terms of B.P. Every link carries a certain weight, and the ANN learns by adjusting them. An ANN can be developed *via* a variety of algorithms, the most well-known of which is the Back Propagation Algorithm, which uses example to learn. After giving an example of what is anticipated from the network throughout training, it automatically updates each weight of the network to generate the appropriate outputs. One statistical error evaluation method that can be used to find mistakes made during the learning process is Mean Squared Error (MSE). Within the range of 0 to 1, the values of the input and output layers are normalized. As seen in Figure 14, a neural network system consists of three layers: The

**Table 4.** Brake power validation test results

| SR. No. | Equation of Regression Obtained with the Use of Taguchi L9 Experiments | Pressure Value by Predicated | Load Value by Predicated | Brake Power by Using Equation | Brake Power by Using Experiment |
|---|---|---|---|---|---|
| 1 | Mean of BP = 0.0473 + 0.0188 pressure + 0.306 load | 6 | 1.5 | 0.618 | 0.6257 |
| 2 | | 5.5 | 1.5 | 0.6077 | 0.6153 |
| 3 | | 5 | 1.5 | 0.5984 | 0.6004 |
| 4 | | 4.5 | 1.5 | 0.5890 | 0.5865 |
| 5 | | 4 | 1.5 | 0.5797 | 0.5681 |
| 6 | | 6 | 2 | 0.7697 | 0.7849 |
| 7 | | 5.5 | 2 | 0.7602 | 0.7619 |
| 8 | | 5 | 2 | 0.7509 | 0.7603 |
| 9 | | 4.5 | 2 | 0.7414 | 0.7388 |
| 10 | | 4 | 2 | 0.7322 | 0.7310 |
| 11 | | 6 | 2.5 | 0.923 | 0.9236 |
| 12 | | 5.5 | 2.5 | 0.9127 | 0.9178 |
| 13 | | 5 | 2.5 | 0.9034 | 0.9082 |
| 14 | | 4.5 | 2.5 | 0.8940 | 0.8947 |
| 15 | | 4 | 2.5 | 0.8849 | 0.8851 |
| Unit | | kg/cm$^2$ | Kg | KW | KW |

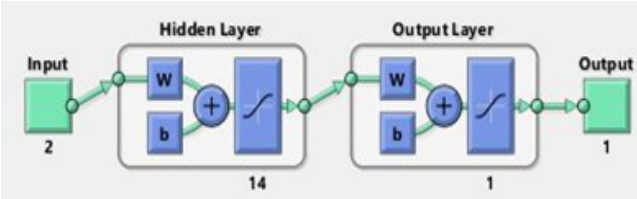



**Figure 14.** Schematic illustration of ANN.

input layer, the layer that is hidden, and the output layer. The input layer has two input elements, followed by an undetectable layer that analyzes information coming from the input element layer, and ultimately a final output layer that decides the result[33].

## 4.7 The Adoption Procedure for ANN

The neural network model for the estimation issue requires three sequential stages: The learning process or training stage, the testing method, and the development of the algorithm or the design of the networks, neural network architecture. In the beginning the networks structure is created. Next, the networks weights, biases, and activation functions are selected. The training algorithms parameters, such as the maximum number of epochs (iterations) and the error goal, are also defined. The training algorithm is then invoked. The first step in testing the outcome after the neural network has been determined is to simulate the neural networks output using the measured input data. The measured outputs are contrasted with this. Independent data must be used for the final validation[34,35]. The study conducted experimental tests to assess the efficiency of compressed air engines across different load levels and air pressures. MATLAB R2021B was utilized to develop the Artificial Neural Network (ANN) model for the study. The input data for the ANN was normalized within the range of (0, 1), using Equation (1) for data normalization.

$$Xn = (Xi - Xmin)/ (Xmax - Xmin) \quad (1)$$

Where Xn = normalized data; Xi = signifies the data intended for normalization; Xmin = denotes the data with the minimum value of the input parameter; Xmax = represents the data with the highest value of the input parameter[36].

Air pressure and load, which is linked to two neurons in the input layer, were the models inputs. In the output layer, one neuron was represented by the output B.P. Equation (2) defined the activation function of the single hidden layer, which was tan sigmoid. In the output layer, it is linear. The layer of hidden neurons were eventually fixed at position 14 by trial and error since their mean squared error value was the lowest among them.

$$y_j = \frac{1}{1 + e^{v_j}} \quad (2)$$

Where yj denotes the output of the neuron and vj indicates the net internal activity of neuron j. Since the Lavenberg-Marquardt back propagation method may produce the best R2, least standard deviations, and means squared errors when compared to other algorithms, it was used in the training process. It is implemented using a training function that converges faster than all other algorithms because it requires fewer epochs with the lowest mean square errors[37,38]. The data utilized in the ANN model was randomly separated into three distinct groups: Testing, validation, and training data. The remaining data was separated into two sets, each containing 12.5% of the total, to be used as testing and validating sets. The remaining 75% of the information was used to train the network[39]. The MSE objective was set at 0.001, with a maximum of 1000 epochs. When any of the performance targets were fulfilled, or the validation error was larger than the test's error, the training was ended[31,40]. Equation (3) illustrates how the Mean Squared Error (MSE), the training algorithm's performance index, is calculated[41].

$$MSE = \frac{1}{N}\left[\sum_{i=1}^{n}(y_i - y_k)^2\right] \quad (3)$$

Where N is the number of patterns, yi is the $i^{th}$ pattern's predicted value, and yk is its target value.

Another way to evaluate the validity of the ANN model is to look at the coefficient of determination (R) between the experimental and predicted values[40]. An ANN's predicted values and the target have a close relationship if the R-value is close to 1.

## 4.8 The Adoption Procedure for ANN

The model was evaluated for the input variables of the air engine, namely load and air pressure, which led to the development of graphs demonstrating the mean square

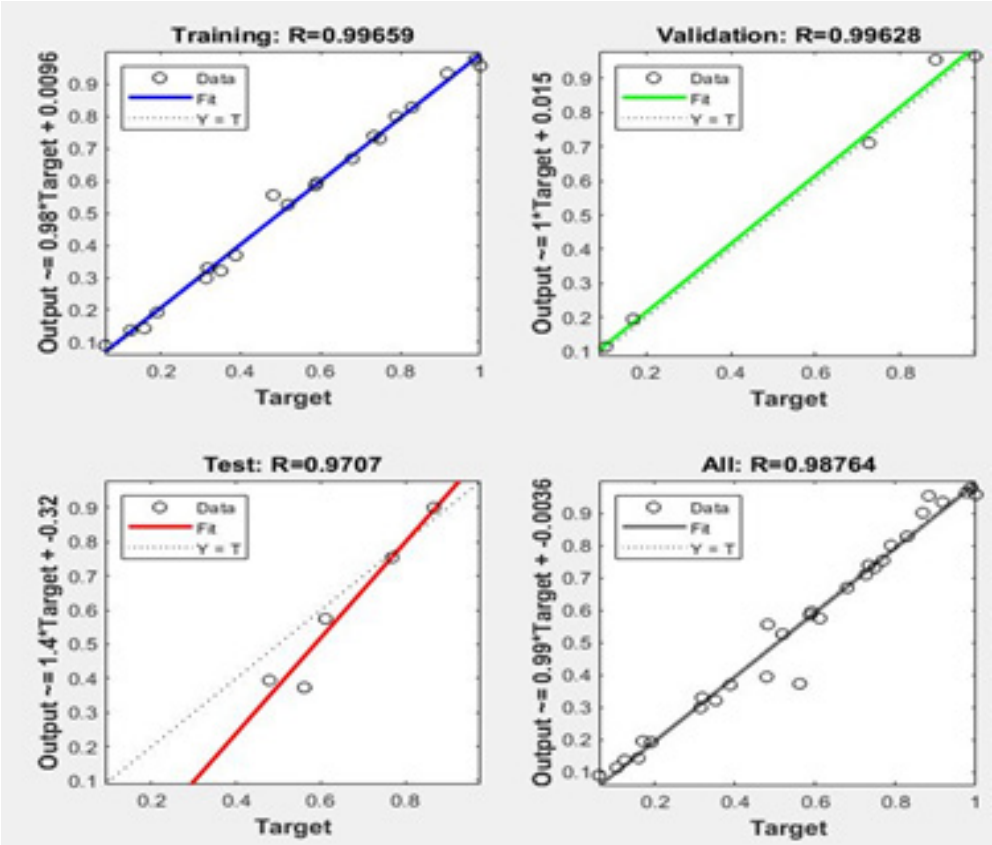



**Figure 15.** Regression plot of air engine brake power by using ANN.

**Table 5.** Comparison with normalized break power and break power obtained using ANN

| SR. No | Pressure | Load | B.P (Experiment) | P-Normalized | Load-Normalized | BP-Normalized (Experiment) | BP-ANN |
|---|---|---|---|---|---|---|---|
| 1 | 4 | 1.5 | 0.5680 | 0 | 0 | 0 | 0.0725 |
| 2 | 4 | 2 | 0.7310 | 0 | 0.25 | 0.2144 | 0.0815 |
| 3 | 4 | 2.5 | 0.8851 | 0 | 0.5 | 0.4170 | 0.2336 |
| 4 | 5 | 1.5 | 0.6003 | 0.1429 | 0 | 0.0425 | 0.0838 |
| 5 | 5 | 2 | 0.7603 | 0.1429 | 0.25 | 0.2528 | 0.1241 |
| 6 | 5 | 2.5 | 0.9082 | 0.1429 | 0.5 | 0.4474 | 0.4792 |
| 7 | 6 | 1.5 | 0.6258 | 0.2858 | 0 | 0.0759 | 0.0925 |
| 8 | 6 | 2 | 0.7849 | 0.2858 | 0.25 | 0.2852 | 0.1637 |
| 9 | 6 | 2 .5 | 0.9236 | 0.2858 | 0.5 | 0.4677 | 0.6025 |
| 10 | 6 | 3 | 1.0644 | 0.2857 | 0.75 | 0.6528 | 0.6243 |
| Units | $Kg/cm^2$ | kg | KW | | | KW | KW |

error and correlation factor. The regression analysis correlation coefficients between corresponding targets and network responses are 0.99659, 0.9707, 0.99628, and 0.98764 for training, testing, validation, and all, respectively, according to Figure 15. In the training dataset, a stronger correlation was attained due to the more even distribution of data points along the regression line[42]. Table 5 displays the ANN predictions for the air engine's B.P. performance. The correlation coefficient for BP is 0.98764, indicating a strong relationship between the expected and predicted outputs. This value is extremely close to one.

## 5.0 Conclusions

The present study follows the DOE L9 approach. Experimental investigations are conducted on an air engine test rig, which is an adapted version of the 4-stroke internal combustion engine, considering three distinct pressure values (4 bar, 5 bar, and 6 bar) and three distinct load values (1.5 kg, 2 kg, and 2.5 kg). Graphs are generated from experimental observations, and the outcomes concerning different responses are thoroughly analyzed and discussed. The following conclusions have been drawn from the data: When it comes to break power, load is more important than air pressure. The combination of a 2.5 kg load and 5 bar pressure is linked to a higher brake power. The Taguchi method provides an efficient methodology in this study to determine the optimal performance output for any given machine. The following findings are drawn after all experiment-based results for speed, mass flow rate, and brake power have been validated in relation to predicted values of load ranges between 1.5 and 2.5 kg and compressed air pressure values between 4 and 6 kg/cm$^2$.

1. Since the R2 values are near unity, the brake power values obtained from the experiment and the equation are consistent with one another.

2. In the event that a 1.5 kg load is applied with a specified air pressure of 4 kg/cm$^2$, the highest possible error between the experiment and equation is found to be about two percent for brake power on a four- stroke single air engine test rig.

3. In the above ANN, there is no difference between the normalized brake power value obtained through equation and the one obtained through experiment.

In conclusion, the afore mentioned findings support the development of single-cylinder compressed air engines as a potential future internal combustion engine substitute. Because the engine heats up less, lighter engines can be built. This could be a significant step toward recycling scrap engines and creating an environment free of pollution. This tackles the issues of pollution and the fuel crisis. The significant value of compressed air pressure and desired output or performance characteristics are obtained through the process parameter optimization for engines using air compressed. All performance characteristics in this study were within the permissible bound, making it highly useful from a technical and commercial viability standpoint.

## 6.0 References


1. Mahato AK, Sharma D, Durga B, Shrestha MN, Bhatt N, Koirala R. Design and development of compressed air engine. JEIS. 2023; 2(1):13-25. https://doi.org/10.3126/joeis.v2i1.50326, 13-25
2. Liang J, Yao B, Xu Y, Zhang H, Yang F, Yang A, *et al.* Experimental research on performance comparison of compressed air engine under different operation modes. Energies. 2023; 16(3):1312. https://doi.org/10.3390/en16031312
3. Wang L, Zhu SL, Zhang XR, Zhang H. Another way of cleaner public transportation: Four-stroke high torque CAE (Compressed Air Engine) performance analysis and CAE bus. Energy Rep. 2022; 8:5727-5738. https://doi.org/10.1016/j.egyr.2022.04.024
4. Li Y, Chen H, Zhang X, Tan C, Ding Y. Renewable energy carriers: Hydrogen or liquid air or nitrogen? Appl Therm Eng. 2010; 30(14-15):1985-1990. https://doi.org/10.1016/j.applthermaleng.2010.04.033
5. Shi Y, Wu T, Cai M, Wang Y, Xu W. Energy conversion characteristics of a hydropneumatic transformer in a sustainable-energy vehicle. Appl Energy. 2016; 171:77-85. https://doi:10.1016/j.apenergy.2016.03.034
6. Xu Y, Wang X, Zhang H, Yang F, Liang J, Yang H, *et al.* Experimental investigation of the output performance of compressed-air-powered vehicles with a pneumatic motor. Sust. 2022; 14(22):15377. https://doi.org/10.3390/su142215377
7. Chang J, Li Z, Huang Y, Yu X, Jiang R, Huang R, *et al.* Multi-objective optimization of a novel combined cooling, dehumidification and power system using

improved M-PSO algorithm. Energy. 2022; 239:122487. https://doi.org/10.1016/j.en ergy.2021.122487
8. Ibrahim ID, Sadiku ER, Jamiru T, Hamam Y, Alayli Y, Eze AA. Prospects of nanostructured composite materials for energy harvesting and storage. J King Saud Univ Sci. 2020; 32(1):758-764. https://doi.org/10.1016/j.jksus.2019.01.006
9. Shen YT, Hwang YR. Design and implementation of an air-powered motorcycles. Appl Energy. 2009; 86(7-8):1105-1110.https://doi.org/10.1016/j.apenergy.2008.06.008
10. Shafiee S, Topal E. When will fossil fuel reserves be diminished? EP. 2009; 37(1):181-189. https://doi.org/10.1016/j.enpol.2008.08.016
11. Shi Y, Wang Y, Liang H, Cai M. Power characteristics of a new kind of air-powered vehicle. Int J Energy Res. 2016; 40(8):1112-1121. https://doi.org/10.1002/er.3507
12. Liu C, You JJ, Sung CK, Huang CN. Modified intake and exhaust system for piston-type compressed air engines. Energy. 2015; 90(1):516-524. https://doi.org/10.1016/j.energy.2015.07.085
13. Renewable energy has been one of the bright spots for the struggling. Available from: https://www.ucsusa.org/sites/default/files/2019-09/Clean-Power-Green-Jobs-25-RES.pdf
14. U.S. Energy Information Administration. How much of U.S. carbon dioxide emissions are associated with electricity generation? FAQ - U.S. Energy Information Administration (EIA); 2023. https://www.eia.gov/tools/faqs/faq.php?id=77&t=11
15. Cai M, Wang Y, Shi Y, Liang H. Output dynamic control of a late model sustainable energy automobile system with nonlinearity. Adv Mech Eng. 2016; 8(11). https://doi:10.1177/1687814016672784
16. Chan CC. The state of the art of electric, hybrid, and fuel cell vehicles. Proc IEEE. 2007; 95(4):704-718. https://doi:10.1109/JPROC.2007.892489
17. Hwang HT, Varma A. Hydrogen storage for fuel cell vehicles. Curr Opin Chem Eng. 2014; 5:42-48. https://doi.org/10.1016/j.coche.2014.04.004
18. Chen H, Ding Y, Li Y, Zhang X, Tan C. Air fuelled zero emission road transportation: A comparative study. Appl Energy. 2011; 88(1):337-342. https://doi.org/10.1016/j.apenergy.2010.07.002
19. Shi Y, Li F, Cai M, Yu Q. Literature review: Present state and future trends of air-powered vehicles. JRSE. 2016; 8(2):025704. https://doi.org/10.1063/1.4944970
20. Xu Q, Cai M, Shi Y. Dynamic heat transfer model for temperature drop analysis and heat exchange system design of the air-powered engine system. Energy. 2014; 68:877-885. https://doi.org/10.1016/j.energy.2014.02.102
21. Motor Development International (MDI). Available from: https://www.mdi.lu/airpod-2-0
22. Liu L, Yu X. Practicality study on air-powered vehicle. Front Energy Power Eng China. 2008; 2(1):14-19. https://doi:10.1007/s11708-008-0004-7
23. Ibrahim H, Ilinca A, Perron J. Energy storage systems-characteristics and comparisons. Renew Sustain Energy Rev. 2008; 12(5):1221-1250. https://doi.org/10.1016/j.rser.2007.01.023
24. Cai M, Kawashima K, Kagawa T. Power assessment of flowing compressed air. J Fluids Eng. 2006; 128(2):402-405. https://doi.org/10.1115/1.2170129
25. Lal A. Design and dynamic analysis of single stroke compressed air engine. 2013; 3(2):315-319.
26. Dudhat RB, Patel NR, Kanadiya VM, Mistry MK, Joshi KM. The investigational study of pragmatic model of compressed air single cylinder engine for increases the performance. Int J Adv Engg Tech. 2013.
27. Simon M, Simon MI. New research and design to obtain a compressed air driven prototype vehicle. Procedia Manuf. 2020; 46:454-460. https://doi.org/10.1016/j.promfg.2020.03.066
28. Montgomery DC. International Student Version, 8th edition. Wiley; 2013. p. 450-455.
29. Aherwar A, Unune D, Pathri B, kishan J. Statistical and regression analysis of vibration of carbon steel cutting tool for turning of EN24 steel using design of experiments. IJMECH. 2014; 3(3):137-151. https://doi:10.14810/ijmech.2014.3312
30. Al-Refaie A, Al-Durgham L, Bata N. Optimal parameter design by regression technique and grey relational analysis. 2010; 3(1).
31. Bilgili M, Sahin B. Comparative analysis of regression and artificial neural network models for wind speed prediction. Meteorol Atmos Phys. 2010; 109(1-2):61-72. https://doi:10.1007/s00703-010-0093-9
32. Kumar S, Pai PS, Rao BRS, Vijay GS. Prediction of performance and emission characteristics in a biodiesel engine using WCO ester: A comparative study of neural networks. Soft Comput. 2015; 20(7):2665-2676. https://doi:10.1007/s00500-015-1666-9
33. Javed S, Murthy YVVS, Baig RU, Rao DP. Development of ANN model for prediction of performance and emission characteristics of hydrogen dual fueled diesel engine with Jatropha methyl ester biodiesel blends. J Nat

Gas Sci Eng. 2015; 26:549-557. https://doi.org/10.1016/j.jngse.2015.06.041

34. Oguz H, Sarıtas I, Baydan HE. Prediction of diesel engine performance using biofuels with artificial neural network. Expert Syst Appl. 2010; 37(9):6579-6586. https://doi.org/10.1016/j.eswa.2010.02.128
35. Bilgili M, Ozgoren M. Daily total global solar radiation modeling from several meteorological data. Meteorol Atmos Phys. 2011; 112(3-4):125-138. https://doi:10.1007/s00703-011-0137-9
36. Cirak B, Demirtas S. An application of artificial neural network for predicting engine torque in a biodiesel engine. AJER. 2014; 2(4):74-80. https://doi.org/10.12691/ajer-2-4-1
37. Channapattana SV, Pawar AA, Kamble PG. Optimisation of operating parameters of DI-CI engine fueled with second generation bio-fuel and development of ANN based prediction model. Appl Energy. 2017; 187:84-95. https://doi:10.1016/j.apenergy.2016.11.030
38. Badday AS, Abdullah AZ, Lee KT. Artificial neural network approach for modeling of ultrasound-assisted transesterification process of crude Jatropha oil catalyzed by heteropolyacid based catalyst. Chem Eng Process. 2014; 75:31-37. https://doi:10.1016/j.cep.2013.10.008
39. Sharma A, Sahoo PK, Tripathi RK, Meher LC. Artificial neural network-based prediction of performance and emission characteristics of CI engine using polanga as a biodiesel. Int J Ambient Energy. 2016; 37(6):559-570. https://doi:10.1080/01430750.2015.1023466
40. Thakur AK, Mer KKS, Kaviti A. An artificial neural network approach to predict the performance and exhaust emissions of a gasoline engine using ethanol-gasoline blended fuels. Biofuels. 2017; 9(3):379-393. https://doi:10.1080/17597269.2016.1271630
41. Phan MC, Beale MH, Hagan MT. A procedure for training recurrent networks. IJCNN. IEEE. 2013: pp.1-8. https://doi.org/10.1109/ijcnn.2013.6706994
42. Saraee HS, Taghavifar H, Jafarmadar S. Experimental and numerical consideration of the effect of $CeO_2$ nanoparticles on diesel engine performance and exhaust emission with the aid of artificial neural network. Appl Therm Eng. 2017; 113:663-672. https://doi.org/10.1016/j.applthermaleng.2016.11.044